Local Anesthetics and Antipsychotic Phenothiazines Interact Nonspecifically with Membranes and Inhibit Hexose Transporters in Yeast

Yukifumi Uesono,*,[1] Akio Toh-e,[†] Yoshiko Kikuchi,[‡] Tomoyuki Araki,[§] Takushi Hachiya,* Chihiro K. Watanabe,* Ko Noguchi, and Ichiro Terashima***

*Department of Biological Sciences, Graduate School of Science, The University of Tokyo, 113-0033 Japan, [†]Medical Mycology Research Center (MMRC), Chiba University, Chiba, 260-8673 Japan, [‡]Department of Life Science, Gakushuin University, Tokyo, 171-8588 Japan, [§]Department of Molecular Biology, Saitama Medical University, Saitama, 350-0495 Japan, and **School of Life Sciences, Tokyo University of Pharmacy and Life Sciences, Tokyo, 192-0392 Japan

ABSTRACT Action mechanisms of anesthetics remain unclear because of difficulty in explaining how structurally different anesthetics cause similar effects. In *Saccharomyces cerevisiae*, local anesthetics and antipsychotic phenothiazines induced responses similar to those caused by glucose starvation, and they eventually inhibited cell growth. These drugs inhibited glucose uptake, but additional glucose conferred resistance to their effects; hence, the primary action of the drugs is to cause glucose starvation. In *hxt*^{0} strains with all hexose transporter (*HXT*) genes deleted, a strain harboring a single copy of *HXT1* (HXT1s) was more sensitive to tetracaine than a strain harboring multiple copies (HXT1m), which indicates that quantitative reduction of *HXT1* increases tetracaine sensitivity. However, additional glucose rather than the overexpression of *HXT1*/*2* conferred tetracaine resistance to wild-type yeast; therefore, Hxts that actively transport hexoses apparently confer tetracaine resistance. Additional glucose alleviated sensitivity to local anesthetics and phenothiazines in the HXT1m strain but not the HXT1s strain; thus, the glucose-induced effects required a certain amount of Hxt1. At low concentrations, fluorescent phenothiazines were distributed in various membranes. At higher concentrations, they destroyed the membranes and thereby delocalized Hxt1-GFP from the plasma membrane, similar to local anesthetics. These results suggest that the aforementioned drugs affect various membrane targets via nonspecific interactions with membranes. However, the drugs preferentially inhibit the function of abundant Hxts, resulting in glucose starvation. When Hxts are scarce, this preference is lost, thereby mitigating the alleviation by additional glucose. These results provide a mechanism that explains how different compounds induce similar effects based on lipid theory.

KEYWORDS anesthesia; glucose transport; membrane lipid; actin; lipid theory

ANESTHETICS have been used clinically for over 160 years, but their mechanism of action remains unclear because of difficulty in explaining why anesthetics with widely varying structures can cause similar effects (Urban *et al.* 2006). Lipid and protein theories have been proposed to explain the mechanism and have been debated for many years (Antkowiak 2001). The lipid theory was proposed to explain the Meyer-Overton rule, which states that the anesthetic potency of various anesthetics correlates with their lipophilicity (hydrophobicity), and it assumes that membrane lipids are the hydrophobic sites of nonspecific interactions with anesthetics (Meyer 1899). However, this theory does not explain why nonspecific interactions with membranes that affect numerous targets result in a specific phenotype such as anesthesia. Therefore, the protein theory was proposed to explain several other observations, including a contradiction of the Meyer-Overton rule. This theory assumes that anesthetics interact specifically with proteins, and it suggests that specific target proteins have anesthetic-binding pockets of limited size as their hydrophobic sites (Franks and Lieb 1990). To date, numerous neurotransmitter receptors and ion channels have been identified as relevant targets (Antkowiak 2001; Urban *et al.* 2006). Antipsychotic effect has been

doi: 10.1534/genetics.115.183806
Manuscript received October 15, 2015; accepted for publication December 30, 2015; published Early Online January 12, 2016.
[1]Corresponding author: Department of Biological Sciences, Graduate School of Science, The University of Tokyo, 7-3-1 Hongo, Bunkyo-ku, Tokyo 113-0033, Japan. E-mail: uesono@bs.s.u-tokyo.ac.jp

found initially for chlorpromazine (CPZ), a phenothiazine (Laborit *et al.* 1952). A dopamine D_2 receptor was considered to be the target for CPZ at an early stage (Snyder *et al.* 1974), but numerous targets for phenothiazines have now been identified (Prozialeck and Weiss 1982; Ogata *et al.* 1989; Mozrzymas *et al.* 1999). According to the protein theory, the large number of possible targets for anesthetics and phenothiazines raises a question about interactions with specific receptors or channels. Therefore, the mechanisms of action of these clinical drugs remain unclear. One reason why crucial targets cannot be determined is the difficulty in demonstrating correlations between drugs and high-order biological phenomena such as anesthesia and psychiatric effects.

Quaternary ammonium compounds (QACs), which are representative cationic surfactants, have potent antibiotic effects. The destruction of membranes by surfactant activity accounts for the antibiotic-effect mechanism at high concentrations, but the antibiotic-effect mechanism at lower concentrations, where membranes are not destroyed, remains unknown (Wessels and Ingmer 2013). Structures of local anesthetics, phenothiazines, alcohols, and QACs are largely different, but they are all amphiphiles and thus, at high concentrations, have sufficient surfactant-like activity to lyse erythrocytes (Seeman 1972; Sheetz and Singer 1974), model membranes (Kitagawa *et al.* 2004), and the budding yeast *Saccharomyces cerevisiae* (Uesono *et al.* 2008, 2011). This activity accounts for the common toxicity of these compounds at high concentrations. At low concentrations that do not cause cell lysis, these compounds induce similar responses, including the inhibition of both translation initiation and polarization of the actin cytoskeleton, nuclear localization of the stress-responsible transcription factor Msn2, and processing-body (P-body) formation for messenger RNA (mRNA) decay in a dose-dependent manner in yeast (Uesono *et al.* 2008, 2011; Araki *et al.* 2015). Volatile anesthetics (Bruce 1975; Heys *et al.* 1989; Horber *et al.* 1988), local anesthetics (Banerjee and Redman 1977; Wang *et al.* 2011), and phenothiazines (Raghupathy *et al.* 1970; Kumar *et al.* 1991) are known to inhibit protein synthesis in animals at cellular, tissue, and whole-body levels. Because volatile anesthetics inhibit translation initiation in yeast (Palmer *et al.* 2005), inhibition of protein synthesis would be an important response that is common to these compounds irrespective of species. Thus, the question remains: how do these compounds with widely varying structures induce similar effects? We consider that the amphiphilic structure that is common to these compounds, rather than their detailed structures, induces these responses at low concentrations (Uesono 2009).

Monitoring actin polarization is more convenient than analyzing protein synthesis to quantify the rapid drug effects of numerous samples (Figure 1A). The dose-response curves are obtained by plotting the percentages of cells with polarized actin *vs.* the drug concentrations. A half-inhibitory concentration (IC_{50}) of polarized actin serves as a measure of a drug's potency to inhibit intracellular processes, and it makes

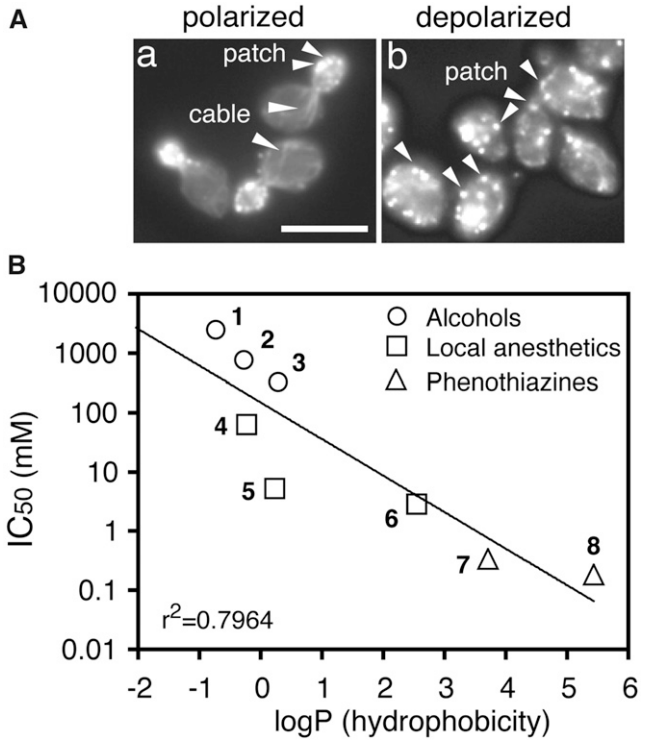

Figure 1 The drug potencies in yeast obey the Meyer-Overton correlation. (A) Representative examples of polarized actin cytoskeletons in wild-type yeast cells (a) and depolarized actins in wild-type cells treated with dibucaine (DC) for 30 min (b) (Uesono *et al.* 2008). Actin cables and patches are indicated by arrowheads. Bar, 10 μm. (B) The half-inhibitory concentrations (IC_{50}) of actin polarization for the indicated water-soluble compounds (Uesono *et al.* 2011) relative to their experimental octanol-water partition coefficients (logP) obtained from the PhysProp Database. The logP values of the compounds are methanol 1, −0.77; ethanol 2, −0.31; 1-propanol 3, 0.25; lidocaine 4, −0.26; tetracaine 5, 0.2; dibucaine 6, 2.52; chlorpromazine 7, 3.69; and trifluoperazine 8, 5.42. The coefficient of determination is indicated in the bottom left of the graph.

pharmacologic analysis possible in yeast (Uesono *et al.* 2011). The experimental octanol-water partition coefficients (logP) serve as a measure of the lipophilicity of the compounds (PhysProp Database, http://esc.syrres.com/fatepointer/search.asp). The correlation between the IC_{50} and logP values of local anesthetics, phenothiazines, and alcohols obeys the Meyer-Overton rule even in yeast (Uesono *et al.* 2011) (Figure 1B). The rule is confirmed in yeast between the growth-inhibitory activities of volatile anesthetics and their lipophilicities (Keil *et al.* 1996), the growth-inhibitory activities of alcohols and their chain lengths (lipophilicity) (Kato and Shibasaki 1980; Kubo *et al.* 1995), and the IC_{50} values of QACs and their chain lengths (Uesono *et al.* 2011). These observations indicate that the mechanism that determines the Meyer-Overton rule, the lipid theory, is conserved in yeast. Thus, an unidentified conserved factor rather than channels or receptors present only in animals would likely be responsible for the mechanism that follows the lipid theory.

Here we demonstrate that local anesthetics and phenothiazines induce the glucose-starvation-mimetic state in yeast

Table 1 Yeast strains used in this study

Strain	Genotype	Sources
BY4741	*MAT***a** *his3Δ1 leu2Δ0 ura3Δ0 met15Δ0*	1
Y03836	BY4741 *rgt2Δ::kanMX4*	1
Y07201	BY4741 *snf3Δ::kanMX4*	1
YRS23	BY4741 *rgt2Δ::kanMX4 snf3Δ::kanMX4*	2
Y06902	BY4741 *grr1Δ::kanMX4*	1
Y04887	BY4741 *rgt1Δ::kanMX4*	1
Y07161	BY4741 *ssn6Δ::kanMX4*	1
Y03731	BY4741 *gpr1Δ::kanMX4*	1
Y00152	BY4741 *gpa2Δ::kanMX4*	1
EBY.S7	*MAT***a** *hxt1-17Δ gal2Δ agt1Δ stl1Δ leu2-3, 112 ura3-52 trp1-289 his3-Δ1 MAL2-8^c SUC2 fgy1-1*	3
YYU608	BY4741 *hxt1::HXT1-GFP::URA3*	4
YYU609	BY4741 *hxt2::HXT2-GFP::URA3*	4

Sources of strains listed: 1, EUROSCARF collection; 2, Uesono *et al.* 2004; 3, Wieczorke *et al.* 2003; 4, this study.

and show that hexose transporters (Hxts) are the common targets of these drugs. In addition, we describe a mechanism that determines how the nonspecific interactions of the drugs having various structures with membrane preferentially induce glucose starvation by targeting abundant Hxts. Finally, we describe a way for alleviating drug-induced cytotoxicity.

Materials and Methods

Strains, media, chemicals, growth conditions, and plasmids

Standard genetic manipulation of yeast and DNA manipulation were performed as described previously (Guthrie and Fink 1991). The strains are listed in Table 1. The media used in this study included YP (2% polypeptone, 1% yeast extract), YPD (YP containing 2% glucose), SD (0.67% yeast nitrogen base, 2% glucose), and SM (0.67% yeast nitrogen base, 2% maltose). Hydrochloride salts of local anesthetics (*e.g.*, tetracaine, lidocaine, procaine, and dibucaine), antipsychotic phenothiazines (*e.g.*, chlorpromazine and trifluoperazine), 3-O-methyl-D-glucose (OMG), 2-deoxy-D-galactose (dGal), and G418 disulfate salts were purchased from Sigma-Aldrich (St. Louis, MO). Lauryltrimethylammonium chloride (TMA12), sodium dodecyl sulfate (SDS), and cycloheximide (CYH) were purchased from Wako Pure Chemicals (Tokyo, Japan). Sodium phosphate buffer (pH 6.0) and Tris-HCl buffer (pH 7.5) were added to all the media at a final concentration of 10 mM to avoid the pH change induced by drugs and growth. Excessive amounts of histidine, methionine, uracil (each 100 μg/ml), and leucine (150 μg/ml) were added to YPD as the final concentrations (5× aa). CYH was added to the culture at a final concentration of 0.3 mM. Yeast cell growth (A_{600}) was monitored by UV spectrophotometer (Amersham Ultrospec 1100 Pro). Another spectrophotometer (Shimazu UV160A) was used for pulse labeling and lysis assays. Ninety-six-well microtiter plates (Corning, NY) were used to test the drug sensitivity of the yeast growth. In brief, logarithmically growing cells (5×10^5 cells) were transferred to each well containing medium and drugs at a total volume of 100 μl, respectively, and incubated for the indicated time at 25°. For construction of the plasmids pHXT1s and pHXT2s, 2.3-kb *Sph*I fragments (*ADH1* promoter–driven *HXT1* or *HXT2*) in Hxt1mnx-pVT and Hxt2mnx-pVT (Kasahara and Kasahara 2003) were inserted into YCplac33 (Gietz and Sugino 1988), respectively. The plasmids used in this study are listed in Table 2.

Measurement of glucose uptake by pulse-labeling assay

Logarithmic cultures ($OD_{600} = 0.3$; 1×10^7 cells/ml, Shimazu UV160A) in YPD (pH 6.0) were treated with the drugs at the indicated concentrations at 25°. At the indicated times, 300 μl of the cultures was removed, and 200 μl was pulse labeled with 1.2 μCi of D-[U-^{14}C]glucose for 7 min at 25° (Amersham), and another 100 μl was measured for OD_{600}. The reaction mixture was collected on a GF/B filter and then washed with an excess amount of water at room temperature. The cell-associated counts were quantified using a Beckman LS6000IC liquid scintillation counter. The uptake rates were calculated as the cell-associated counts/(A_{600}·minute) at the indicated times (Uesono and Toh-e 2002).

Microscopic analysis

Actin staining and calculation of the percentages of polarization were performed as described previously (Delley and Hall 1999; Uesono *et al.* 2004). One milliliter of logarithmic cultures ($OD_{600} = 0.7$; 1×10^7 cells/ml, Ultrospec 1100 Pro) in YPD (pH 6.0) was treated with the indicated drugs. Cultures (100–200 μl) grown under the indicated conditions were fixed by adding formaldehyde to a culture at a final concentration of 5%, washed twice with phosphate-buffered saline, and then stained with rhodamine phalloidin (Molecular Probes, Eugene, OR). The percentages of polarization were calculated as the fraction of cells exhibiting a polarized actin cytoskeleton in small- and medium-budded cells ($n > 300$). Cells with <50% of their actin patches in the bud were considered to have a depolarized actin cytoskeleton. For the detection of phenothiazines (De Filippi *et al.* 2007) and GFP-tagged Hxts (Yoshida *et al.* 2012), logarithmic cultures of the BY4741 strains expressing *HXT1-GFP* and *HXT2-GFP* in

Table 2 Plasmids used in this study

Plasmid	Description	Sources
pHXT1m (Hxt1mnx-pVT)	pVT102-U (*2μ ori*, *URA3*) backbone, *ADH1*p-driven *HXT1*	1
pHXT2m (Hxt2mnx-pVT)	pVT102-U (*2μ ori*, *URA3*) backbone, *ADH1*p-driven *HXT2*	1
pHXT1s	YCplac33 (*ARS1*, *CEN4*, *URA3*) backbone, *ADH1*p-driven *HXT1*	2
pHXT2s	YCplac33 (*ARS1*, *CEN4*, *URA3*) backbone, *ADH1*p-driven *HXT2*	2
pHXT1-GFP	pRS306 (integrate-type, *URA3*) backbone, for replacement of endogenous *HXT1* with *HXT1-GFP*	3
pHXT2-GFP	pRS306 (integrate-type, *URA3*) backbone, for replacement of endogenous *HXT2* with *HXT2-GFP*	3

Sources of plasmids listed: 1. Kasahara and Kasahara 2003; 2, this study; 3, Yoshida *et al.* 2012.

YPD (pH 6.0) were treated with the indicated drugs. The fluorescence signals for phenothiazine detected by UV excitation (330–385 nm) were immediately recorded before changing their colors. Images were recorded using an Olympus BX50 microscope with a DP71 CCD camera using DP controller software (Olympus, Tokyo, Japan). Olympus U-MWU, U-MWIG, and U-MWIB/GFP cubes were used to detect phenothiazines, actin, and GFP, respectively.

Lysis assay

Alkaline phosphatase (ALP) activity was determined as described previously (Toh-e *et al.* 1976; Uesono *et al.* 2011). Because mature ALP is localized in the vacuoles, the activity is detected in the cells permeabilized by clinical drugs but not in living cells without the drugs. Logarithmic cultures (OD_{600} = 0.3; 1×10^7 cells/ml, Shimazu UV160A) in YPD (pH 6.0) were treated with the drugs for the indicated times. The cultures (100 μl) were mixed with 300 μl of reaction mixture containing 50 mM Tris-HCl (pH 9.0) and 5 mM $MgSO_4$, and 100 μl of 3.2 mg/ml *p*-nitrophenylphosphate (*p*-NPP, Wako, Osaka, Japan) was added to start the reaction. Cells were incubated at 35° for 10–60 min, and then reactions were stopped by the addition of 250 μl of 20% trichloroacetic acid, followed by 750 μl of 1 M Na_2CO_3. Liberated *p*-nitrophenol was measured spectrophotometrically at A_{420} nm, and the specific activity (A_{420} nm/A_{600} nm) was calculated as $[A_{420} - A_{420}\ (C)] \times 0.25/[\text{time (min)} \times A_{600}]$. A_{420} (C) indicates the value of the YPD solution without cells.

Polysome analysis

Polysome analysis was carried out as described previously (Araki *et al.* 2015). Logarithmic cultures (1×10^7 cells/ml) grown in 40 ml of YPD (pH 6.0) were treated with the indicated drugs and used for polysome analysis. Lysates equivalent to 5 A_{260} units were prepared in the presence of CYH (0.3 mM) and were layered onto 11 ml of a continuous 10–45% sucrose gradient, and then ultracentrifugation was performed using a p40ST rotor (Himac CP80MX, Hitachi, Tokyo, Japan) at 35,000 rpm for 2.5 hr at 4°. Gradients were fractionated using an ALC automatic liquid charger (Advantec, Tokyo, Japan) and detected at 254 nm with a UV-1I monitor system (Amersham, Piscataway, NJ). The polysome/monosome ratio was determined as the ratio of the area of polysomes to the area of 80S monosomes using ImageJ (developed and maintained by the National Institutes of Health, Bethesda, MD).

Viability

Early logarithmic cultures (4×10^6 cells/ml, 500 μl) were treated with 2.5 mM TC for 4 hr with shaking at 25°. The diluted cultures were spread onto YPD plates at 25° for 3 days. Viabilities were determined as colony-forming units (CFUs) by counting cell numbers in a hemacytometer and comparing them with colony numbers on YPD plates.

Halo assay

Logarithmic cultures (2×10^5 cells) of BY4741 were mixed with 4 ml of YPD (pH 7.5, 1% agar) containing 2 or 8% glucose and then layered onto the YPD plates (pH 7.5, 2% agar) containing the same concentrations of glucose. Drug solution (3 μl) at the indicated concentration was dripped onto a disk filter that was placed on each plate and incubated for 2 days at 25°. The drug solution is ~100 times the concentration of the IC_{50} determined by actin polarization (Uesono *et al.* 2011).

Data availability

Strains and constructs described in this paper are available on request.

Results

Local anesthetics and antipsychotic phenothiazine inhibit uptake of glucose

In yeast, local anesthetics [*e.g.*, tetracaine (TC), lidocaine (LC), dibucaine (DC), and procaine (PC)], antipsychotic phenothiazines [*e.g.*, chlorpromazine (CPZ) and trifluoperazine (TFZ)], and a QAC [*i.e.*, lauryltrimethylammonium compound (TMA12)] induce rapid and simultaneous inhibition of both translation initiation and actin polarization, responses that resemble those induced by high salinity and glucose starvation (Uesono *et al.* 2008, 2011). This response is unlikely to be caused by amino acid starvation inhibiting translation initiation without rapid depolarization of actin or by mild heat stress inhibiting actin polarization without translational inhibition (Delley and Hall 1999; Uesono and Toh-e 2002; Uesono *et al.* 2004; Uesono 2009). Thus, it is conceivable that these clinical drugs induce glucose starvation, salt stress, or other responses that inhibit both translation initiation and actin polarization in yeast. Because high salinity stimulates glucose uptake (Uesono and Toh-e 2002), these possible responses can be evaluated by testing

the effects of the drugs on glucose uptake using pulse labeling of [^{14}C]glucose. The uptake rate of [^{14}C]glucose decreased following 30-min treatments with TC, LC, and CPZ at the indicated concentrations (Figure 2A). The uptake rate of [^{14}C]glucose decreased rapidly following treatment with 10 mM TC, whereas it decreased gradually following treatment with 2.5 mM TC (Figure 2B), which indicates that the administration of TC inhibits uptake of glucose in a dose-dependent manner. These results suggest that responses to local anesthetics and phenothiazine occur via glucose starvation.

Additional glucose confers multidrug resistance specific to cationic amphiphiles

Assuming that cationic amphiphiles, such as local anesthetics, phenothiazines, and QACs, nonspecifically interact with amphiphilic membrane lipids, various transporters and channels on membranes would be affected by these drugs. Thus, it is not surprising that they induce glucose starvation by inhibiting the glucose uptake system, *i.e.*, one of their various targets. However, if glucose starvation were crucial for the effects of these drugs, additional glucose likely would alleviate their effects. Thus, we examined whether the addition of excessive amounts of glucose alleviated the growth inhibitions induced by these compounds. The ability of the compounds to inhibit growth can be evaluated by assessing the size of the inhibitory zone in a plate (halo assay), with the exception of LC and PC, which require high concentrations. Because the halo size reflects the potencies of the compounds to inhibit growth, concentrations of the drug were adjusted to form similar sizes of halo (Figure 3A). The halo sizes formed by these compounds in the presence of 8% glucose were smaller than those formed with 2% glucose, except for antibiotic G418 and amphiphilic SDS, which have an anionic sulfate and the same straight alkyl chain (C_{12}) as the TMA12 (Figure 3A). The growth inhibitions caused by LC and PC also were alleviated in the presence of 8% glucose (Figure 3B). Therefore, additional glucose specifically alleviates the growth inhibitions caused by compounds with cationic amphiphilic structures irrespective of the differences in their detailed structures.

Importantly, in the presence of 2% glucose, growth recovery was observed in the halo formed by TMA12 but not in the halo formed by DC, which indicates that TMA12 is less toxic than DC (Figure 3A, left). This is consistent with the idea that the lysis/shutdown ratios of these compounds (TMA12 = 4.2; DC = 0.5), which are considered to be indicators of the safety of the drugs in yeast, function as the therapeutic index (Uesono *et al.* 2011). Thus, the halo assay also can be used to evaluate drug safety. The size of the clear halo formed by DC in the presence of 8% glucose also was smaller than that formed with 2% glucose, which suggests that the toxicity of DC is reduced by additional glucose.

Glucose starvation accounts for the early responses induced by low concentrations of TC

We then examined the effects of additional glucose on the early responses induced by TC. Both actin polarization

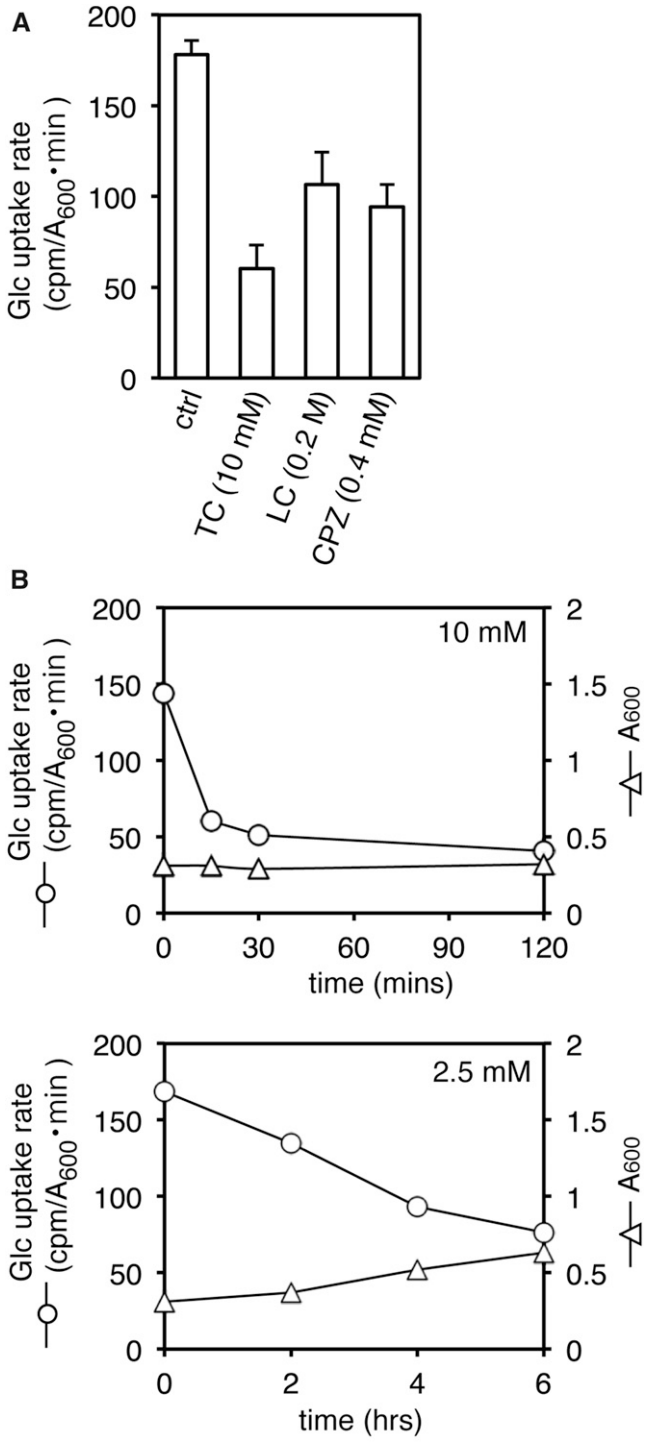

Figure 2 Rates of glucose uptake on treatment with local anesthetics or antipsychotic phenothiazine. (A) The rates of [^{14}C]glucose uptake of BY4741 cells grown in YPD at 30 min after treatment with 10 mM TC (tetracaine), 200 mM LC (lidocaine), and 0.4 mM CPZ (chlorpromazine) or without drug (ctrl) were determined by pulse labeling for 7 min. Error bars represent SD, $n \geq 3$. (B) Early logarithmic cultures (OD_{600} = 0.3) of BY4741 cells grown in YPD (2% Glu, pH 6.0) were treated with 10 mM (top) or 2.5 mM (bottom) of TC at time zero. The rates of [^{14}C]glucose uptake were plotted at the indicated times. Each cell growth was monitored as the OD_{600} of cultures. Representative data from one of three independent experiments are shown.

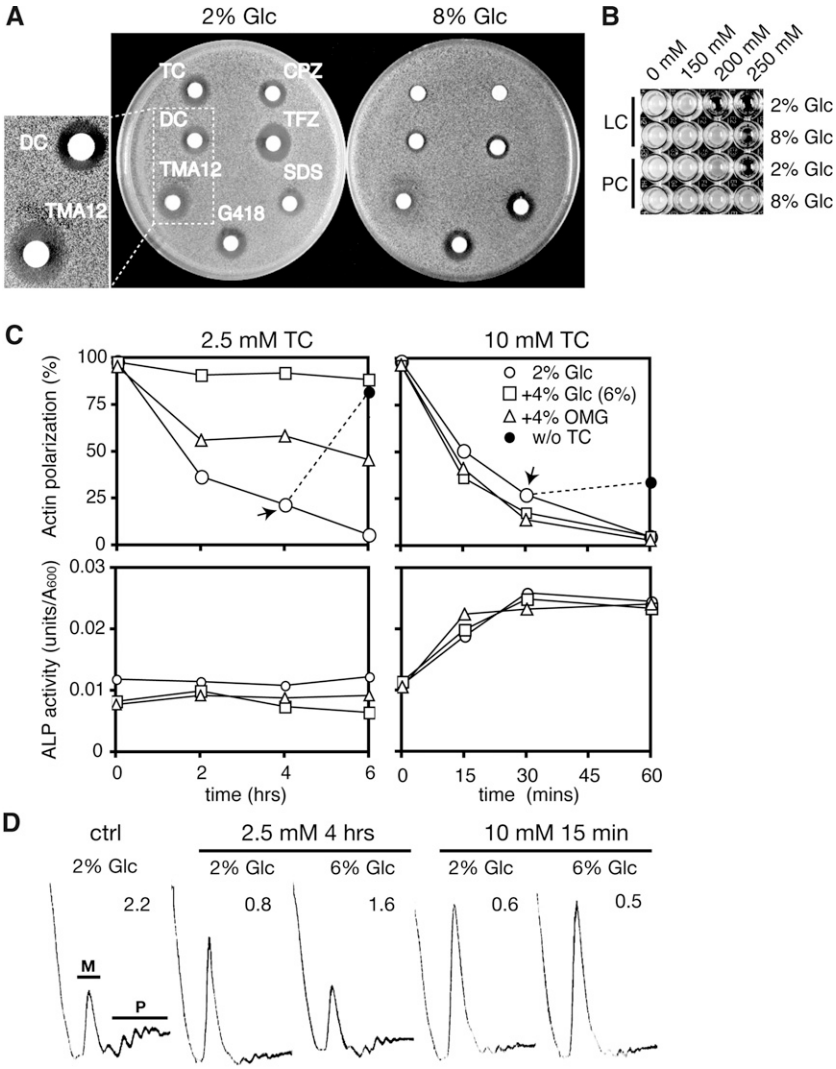

Figure 3 Effects of additional glucose on the growth inhibitions and responses induced by cationic amphiphiles. (A) Logarithmic BY4741 cells were layered onto the YPD plates (pH 7.5) containing 2 or 8% glucose. Filter papers containing 3 μl of the drugs (20 mM CPZ, 20 mM TFZ, 200 mM SDS, 72 mM G418, 10 mM TMA12, 500 mM DC, and 500 mM TC) were put onto each plate and incubated for 2 days at 25°. Close-ups of the halos formed by DC and TMA12 are shown in the left panel. (B) The BY4741 strain was grown for 3 days at 25° on 96-well plates containing YPD (2 or 8% glucose, pH 6.0) supplemented with LC and PC (procaine) at the indicated concentrations. (C) Logarithmic cultures (OD_{600}= 0.7) of BY4741 grown in YPD (2% Glc, pH 6.0) and in YPD supplemented with additional 4% glucose (6% Glc) and 4% methylglucose (2% Glc + 4% OMG) were treated with 2.5 mM (left) or 10 mM (right) of TC at time zero. The percentages of cells with polarized actin (top) and ALP activities (bottom) are indicated, respectively. TC was omitted from the cell cultures containing each concentration of TC at the indicated times (arrows) and then incubated (without tetracaine) (top panels). (D) Logarithmic cultures of BY4741 cells grown in YPD (2 or 6% glucose, pH 6.0) were treated with TC at 2.5 mM for 4 hr or 10 mM for 15 min, and their polysome profiles were analyzed. The polysome/monosome (P/M) ratios are indicated in each panel.

and translation initiation in the cells grown in YPD (2% glucose) were gradually but severely inhibited by 2.5 mM TC within 6 hr (Figure 3, C and D, left), a response that was similar to the timing of the inhibition of glucose uptake caused by 2.5 mM TC (Figure 2B, bottom). Thus, inhibition of the intracellular reactions is correlated with the inhibition of glucose uptake. The severe inhibition of both reactions was not observed in cells grown in YPD containing 6% glucose during the experimental period (Figure 3, C and D, left). These results indicate that glucose starvation is responsible for the early responses induced by TC. We also investigated whether the alleviation of drug effects by additional glucose depended on the metabolism of glucose. Preadministration (4%) of 3-O-methyl-D-glucose (OMG), a nonmetabolizable glucose analogue, weakened depolarization of actin in the cells treated with 2.5 mM TC (Figure 3C, left); this indicates that a mechanism other than glucose metabolism also might contribute to alleviating the effects of drug administration.

Neither additional glucose nor OMG conferred resistance to both the rapid inhibitions induced by 10 mM TC (Figure 3, C and D, right). Therefore, the addition of glucose or a glucose analogue effectively alleviates the responses induced by low drug concentrations, *e.g.*, 2.5 mM TC. Actin polarization recovered to 80% in the budded cells, which was caused by omission of TC from the cells treated with 2.5 mM for 4 hr (Figure 3C, left, black circle); this indicates that the effect of 2.5 mM TC is reversible, similar to the effects of low concentrations of cationic surfactant (Uesono *et al.* 2008). In contrast, actin polarization recovered to just 27% after omission of TC from cells treated with 10 mM for 30 min (Figure 3C, right, black circle), which shows that 10 mM is severely toxic. Based on ALP activity, TC treatment led to rapid cell lysis at 10 mM, possibly via its surfactant activity, but not at 2.5 mM (Figure 3C, bottom) (Araki *et al.* 2015). This suggests that the cell membrane is damaged by 10 mM TC and that membrane damage would not be rescued by additional glucose or OMG. Consequently, glucose starvation accounts for the early responses induced by low concentrations of TC, and the alleviation of drug effects by additional glucose requires the cell membrane to have a normal state.

Additional glucose can partially control the response already induced by the administration of TC

We examined whether additional glucose can affect the TC-induced response by monitoring actin polarization. In comparison with treatment with 2% glucose (Figure 4A, white circles), pretreatment with 6% glucose for 1 hr clearly reduced the rate of actin depolarization in the cells after administration of 2.5 mM TC (Figure 4A, triangles), as shown in Figure 3C (left). This result might have been caused indirectly by preadaptation to TC via the expression of glucose-inducible genes during the administration of additional glucose. In this case, additional glucose would not reduce the rate of actin depolarization in the cells pretreated with TC. However, we found that additional glucose did reduce the rate of actin depolarization at any time after treatment with TC, which suggests that the addition of glucose directly reverses TC-induced depolarization of actin. If glucose and TC act on the actin polarization via competitive binding at the same site, *e.g.*, at a substrate recognition site of Hxt (see later), elimination of TC from the site by excessive amounts of glucose would lead to the repolarization of actin, as observed following omission of TC (Figure 3C, left, black circle). However, we found that additional glucose interrupted the progression of the actin depolarization by TC but did not lead to apparent repolarization at any time (Figure 4A). This indicates that glucose and TC do not act competitively at the same site; indeed, they apparently act at different sites; *i.e.*, glucose interacts with Hxts and TC interacts with membranes (Figure 7). Consequently, additional glucose can partially control the response already induced by the administration of TC at any time.

Additional glucose alleviates the reduction in cell viability caused by TC

Most local anesthetics are known to induce cell death, although the mechanism remains unknown (Werdehausen *et al.* 2009). We found that high concentrations of TC, *e.g.*, 10–20 mM, lysed yeast cells and thereby reduced cell viability (Figure 3C, right, and Figure 7B). A lower concentration of TC, 2.5 mM, did not lyse cells but still caused cell death; indeed, cell viability decreased by approximately 50% after 4 hr of incubation (Figure 4B). Glucose deprivation alone did not reduce cell viability (Figure 4B), but it rapidly and severely inhibited both translation initiation and actin polarization (Ashe *et al.* 2000; Uesono *et al.* 2004); this indicates that the reduction in viability cannot be explained by inhibition of glucose uptake. Thus, TC apparently inhibits another unknown survival process. The reduction in cell viability caused by 2.5 mM TC also was alleviated in the presence of 6% glucose or improved slightly by the addition of 4% OMG (plus 2% glucose), as observed with alleviation of the intracellular inhibitions (Figure 3, C and D, left). Therefore, the reduction in cell viability is not due to undetectable and irreversible membrane disruption caused by the surfactant activity of TC. Collectively, TC appears to induce the glucose-starvation-mimetic state via unknown survival processes and inhibition of glucose uptake, both of which are redundantly required for cell survival.

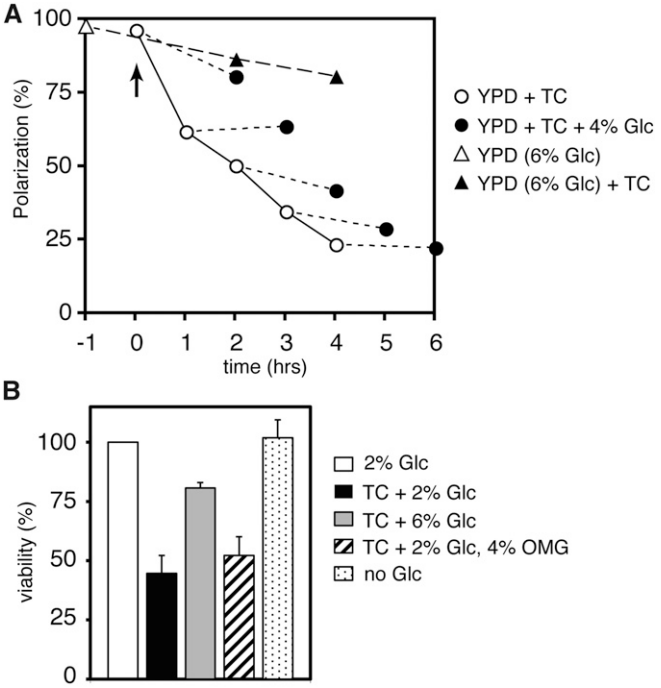

Figure 4 Effects of additional glucose on the timing of actin depolarization and the reduction in viability caused by TC. (A) The percentages of cells with polarized actin in BY4741 cells treated by TC before or after treatment with additional glucose. TC was added to the cell cultures (OD_{600} = 0.7) grown in YPD (2% glucose, pH 6.0) at the final concentration of 2.5 mM (arrow), then the glucose was added to the cultures at a final concentration of 6% at each time point (white circles), and the cultures were further incubated for 2 hr (black circles). Glucose was added to the cell cultures grown in YPD at a final concentration of 6% at 1 hr before treatment with TC (white triangle), then TC was added to the cell cultures (OD_{600} = 0.7) at a final concentration of 2.5 mM (arrow), and the cultures were further incubated for 2–4 hr (black triangle). (B) BY4741 cells (OD_{600} = 0.2) grown in YPD (pH 6.0) (TC + 2% Glc) and in YPD containing additional 4% glucose (TC + 6% Glc) or 4% methylglucose (TC + 2% Glc, 4% OMG) were treated with 2.5 mM TC, and the cells grown in YPD were shifted to YP (no Glc) for 4 hr with shaking, respectively. The CFUs are indicated as a percentage of the cells grown in YPD without TC (2% Glc). Error bars represent SDs, $n \geq 3$

Additional glucose, but not overexpression of HXT1/2, confers resistance to TC

If the Hxts are the targets of the clinical drugs, a reduction or loss of function of Hxts might increase drug sensitivity; conversely, an increase or gain of function of Hxts might confer drug resistance. One of the obstacles to investigating the function of Hxts comes from the fact that 18 genes (*HXT1–17* and *GAL2*) encode Hxts, and their expression is intricately regulated by carbon sources in media (Ozcan and Johnston 1999). First, we examined whether TC sensitivity was affected by carbon sources. The wild-type (WT) strain was more sensitive to TC in media containing a nonfermentable carbon source or polysaccharides rather than monosaccharides.

However, it was difficult to evaluate the correlation between *HXT* gene expressions based on carbon sources and TC sensitivity (data not shown) because the *HXT5–7* genes are expressed even by nonfermentable carbon sources (Liang and Gaber 1996; Ozcan and Johnston 1999). Therefore, we chose to examine TC sensitivity in mutants that affected *HXT* gene expression when they were grown on a medium containing glucose as a sole carbon source (Ozcan and Johnston 1999) (Figure 5A). Rgt2 and Snf3 are the glucose sensors for high and low levels of glucose, respectively, and Grr1 is a component of an SCF ubiquitin ligase complex; these proteins are positively involved in the expression of many *HXT* genes. We found that the *rgt2* and *snf3* disruptants were slightly sensitive to TC and that the *rgt2 snf3* double disruptant was more sensitive than each of the respective single disruptants. The *grr1* disruptant also was sensitive to TC. Rgt1 is a bifunctional transcription factor that is positively involved in the expressions of *HXT* genes at high concentrations of glucose and negatively involved in their expression in the absence of glucose. The *rgt1* disruptant also was slightly sensitive to TC in the presence of 2% glucose. These results suggest that a reduction in *HXT* gene expression increases TC sensitivity. The expressions of many *HXT* genes are greatly increased in the *ssn6* disruptant, which is defective in a general repressor of various genes. However, the *ssn6* disruptant was slightly sensitive to TC rather than being TC resistant, which suggests that an increase in *HXT* expression does not confer TC resistance. Because the *rgt2 snf3*, *grr1*, and *ssn6* disruptants grew slowly even in the absence of TC, the TC sensitivities reported here might not be precise evaluations; thus, alternative evaluations are necessary.

We then investigated whether glucose concentration was crucial for TC sensitivity. Glucose concentrations of <2% increased TC sensitivity, but concentrations >2% conferred TC resistance in a dose-dependent manner (Figure 5B). TC sensitivity caused by lowering glucose concentration is consistent with that caused by decreasing *HXT* gene expression (Figure 5A); this suggests that reduction in Hxt function and the decreased number of Hxts are responsible for the observed TC sensitivity. To determine whether the additional glucose-induced TC resistance depended on *HXT* gene expression, the *HXT1* and *HXT2* genes, which encode low- and high-affinity glucose transporters, were highly expressed under the *ADH1* promoter on multicopy vectors (pHXT1m and pHXT2m) (Kasahara and Kasahara 2003). The WT strains harboring pHXT1m and pHXT2m did not confer TC resistance in the presence of 2% glucose (Figure 5C), as observed in the *ssn6* disruptant (Figure 5A). Although these strains displayed TC resistance in the presence of 6% glucose, this resistance did not increase further following overexpression of *HXT1* and *HXT2*. Because many *HXT* genes are already highly expressed in the WT strain (Ozcan and Johnston 1999), additive *HXT* expression would not further affect TC resistance. Thus, these results suggest that the rate-limiting factor for TC resistance is the amount of substrate for Hxts rather than the number of Hxts.

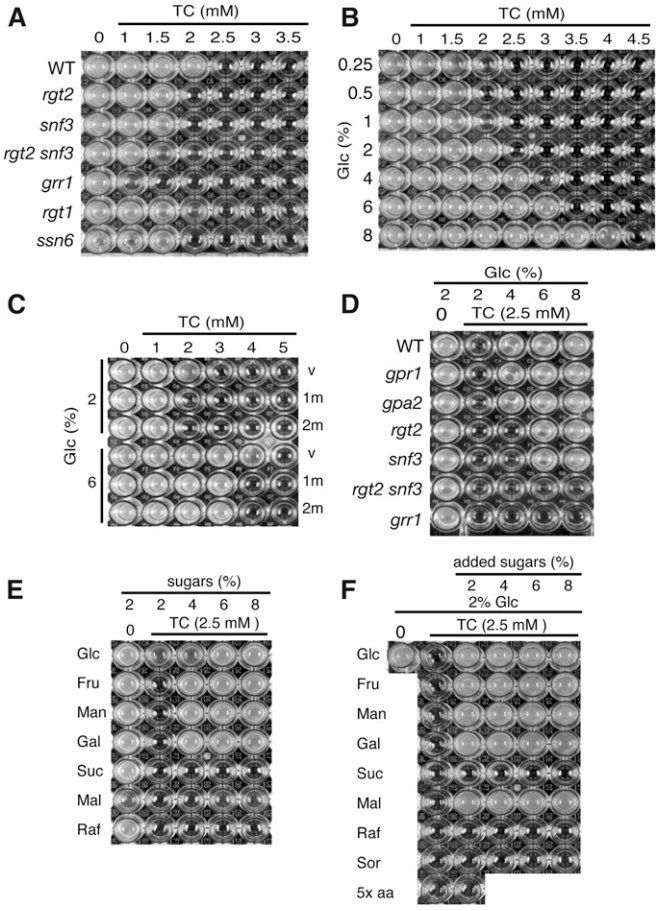

Figure 5 Dose effects of TC and sugars on the growth of mutants defective in *HXT* gene expression. (A) The indicated mutant strains (vertical axis) were incubated on 96-well plates containing YPD (pH 6.0) and TC at the indicated concentrations (horizontal axis). (B) The WT strain (BY4741) was incubated in wells containing YP (pH 6.0) supplemented with glucose (vertical) and TC (horizontal) at the indicated concentrations, respectively. (C) The WT strains harboring YCplac22 (v), pHXT1m (1m), and pHXT2m (2m) precultured in SD-Ura were grown in YPD for 4–5 hr. The strains were incubated in wells containing YP (pH 6.0) supplemented with glucose (vertical axis) and TC (horizontal axis) at the indicated concentrations, respectively. (D) The indicated mutant strains (vertical axis) were incubated in wells containing YP (pH 6.0) supplemented with glucose and TC at the indicated concentrations (horizontal axis), respectively. (E) The WT strain was incubated in wells containing YP (pH 6.0) supplemented with the indicated sugars (glucose, Glc; fructose, Fru; mannose, Man; galactose, Gal; sucrose, Suc; maltose, Mal; and raffinose, Raf) (vertical axis) and TC at the indicated concentrations (horizontal axis). (F) The WT strain was incubated in wells containing YPD (pH 6.0) supplemented with sugars (see in E), sugar alcohols (sorbitol, Sor), and excessive amounts of amino acids and uracil (5× aa) (vertical axis) and TC at the indicated concentrations (horizontal axis). These 96-well plates were incubated at 25° for 3 days (A–D) and 2 days (E and F), respectively.

Additional glucose alleviates TC sensitivity via Rgt2/Snf3 and Grr1

Extracellular glucose is sensed by the Gpr1-Gpa2 system (G-protein-coupled glucose receptor) and the Rgt2-Snf3

glucose sensors, as well as the Hxt system (Gancedo 2008). Hence, excessive amounts of glucose might stimulate the growth of yeast via these hexose-sensing systems. Additional glucose alleviated TC sensitivity at 4–8% in the *gpr1* and *gpa2* disruptants (Figure 5D), which suggests that the Gpr1-Gpa2 system is not required for glucose-induced alleviation of the drug's effects. Additional glucose alleviated TC sensitivity at 6–8% but not at 4% in the *rgt2* and *snf3* disruptants, whereas it did not alleviate TC sensitivity at 4–8% in the *rgt2 snf3* double disruptant. Because apparent growth of the *rgt2 snf3* double disruptant was observed after 3 days in the absence of TC, the inability to restore the growth by additional glucose cannot be attributed to the slow growth of the *rgt2 snf3* double disruptant. These results indicate that the glucose-induced alleviation of TC effects requires the redundant function of both the Rgt2 and Snf3 glucose sensors. Both these glucose sensors positively regulate *HXT* expression via Grr1 (Ozcan and Johnston 1999). If the sensors were involved in the alleviation of effects via targets other than the Grr1-dependent *HXT* expression, additional glucose would alleviate TC sensitivity in the *grr1* disruptant. However, this is not the case, which indicates that alleviation of TC effects requires Grr1. In summary, these observations show that alleviation of TC effects by additional glucose requires the expression of *HXT* genes.

Additional monosaccharides alleviate TC sensitivity

Hxts transport various monosaccharides as well as glucose, but they do not transport polysaccharides. If TC induces Hxt-specific carbon-source starvation, additional monosaccharides other than glucose would specifically alleviate the observed TC sensitivity. As shown in Figure 5E, as a sole carbon source, the addition of excessive amounts of monosaccharides (*e.g.*, glucose, fructose, mannose, and galactose) alleviated TC sensitivity, whereas addition of disaccharide sucrose and trisaccharide raffinose did not. Interestingly, addition of disaccharide maltose at 8% also slightly alleviated TC sensitivity. In the presence of 2% glucose, additional maltose clearly alleviated TC sensitivity, whereas additional sucrose and raffinose did not (Figure 5F). This is so possibly because maltose transporters have structural similarity to Hxts (Cheng and Michels 1989). Because administration of TC stimulated the eIF2α phosphorylation that is induced by amino acid starvation (Araki *et al.* 2015), TC also might induce amino acid starvation. However, administration of excessive amounts of auxotrophic amino acids and uracil did not alleviate the sensitivity to 2.5 mM TC in the presence of 2% glucose, which indicates that amino acid starvation and uracil starvation are not involved in the sensitivity to TC at low concentrations. This finding is in agreement with reports that TC induced eIF2α phosphorylation at 10 mM but not at 2.5 mM (Araki *et al.* 2015). The addition of excessive amounts of sorbitol, a nonfermentable sugar alcohol, did not alleviate TC sensitivity, as observed with other polysaccharides, which indicates that alleviation of the effects of TC is not due to high osmolarity. Collectively, these results suggest that the transporters for monosaccharides and maltose are involved in the sensitivity to TC at low concentrations, but the systems that assimilate other polysaccharides and those for sensing amino acids and osmolarity appear not to be involved.

Additional monosaccharides alleviate sensitivity to the clinical drugs via Hxt1

The Hxts encoded by 18 genes have a similar structure and are functionally redundant; thus, none of the Hxts are essential for growth on glucose (Ozcan and Johnston 1999). This indicates that TC-sensitive growth is not due to the inhibition of a Hxt only. Indeed, when considered individually, the *rgt2* or *snf3* disruptants were defective in the expression of several *HXT* genes and only slightly sensitive to TC, whereas the *rgt2 snf3* double disruptant and the *grr1* disruptant were defective in the expression of many *HXT* genes and severely TC sensitive (Figure 5A). These findings suggest that many *HXT* genes could be redundantly involved in the observed TC sensitivity. However, the expression levels of the 18 *HXT* genes vary depending on the type and amount of the carbon source, and this makes evaluating Hxts based on their drug effects complicated. In addition, because various sugars and the aforementioned mutants would affect the expression of numerous genes, we cannot completely exclude the possibility that TC sensitivity and its alleviation by additional sugars are due to the expression of non-*HXT* genes. To avoid the complicated effects of multiple *HXT* genes and their regulation, we examined the drug effects in the *hxt*^{0} mutant (EBY.S7) (Wieczorke *et al.* 2003), in which all *HXT* genes are deleted but a *HXT* gene is expressed under the same *ADH1* promoter. The *ADH1* promoter–driven *HXT1* and *HXT2* genes were expressed on single-copy vectors (pHXT1s and pHXT2s) or multicopy vectors (pHXT1m and pHXT2m) in the *hxt*^{0} mutant. As shown in Figure 6A, the *hxt*^{0} mutant harboring pHXT1s (HXT1s) was more sensitive to TC than that harboring pHXT1m (HXT1m) for 3 days. Although the HXT1s strain also grew slowly, similar to the *rgt2 snf3* and *grr1* disruptants, the strain was still sensitive to TC at concentrations $>$1.5 mM after 5 days (data not shown). This result indicates that a reduction in *HXT1* expression accounts for TC sensitivity. We could not evaluate the effect of differing levels of Hxt2 because the *hxt*^{0} mutant harboring pHXT2s (HXT2s) grew poorly in the absence of TC for 7 days.

Additional monosaccharides (*e.g.*, glucose, fructose, and mannose) alleviated the sensitivity to TC (2.5 and 3.5 mM) in the HXT1m strain but not in the HXT1s strain (Figure 6B), as observed with the *rgt2 snf3* and *grr1* disruptants (Figure 5D). Additional glucose alleviated the sensitivity to other local anesthetics (*e.g.*, DC and LC) and phenothiazine (CPZ) in the HXT1m strain but not in the HXT1s strain (Figure 6C). These results indicate that additional monosaccharides alleviate the observed clinical drug-induced sensitivities via Hxt1 irrespective of the drug structures. Additional glucose alleviated the sensitivity to TMA12 in the WT strain (Figure 3A)

but not in the HXT1m or HXT1s strain (Figure 6C); this suggests that other Hxts might be involved in the sensitivity to TMA12.

Nonmetabolizable hexose analogues alleviate TC sensitivity via Hxt1

The Hxts have different substrate specificities to monosaccharides (Leandro *et al.* 2009). In a WT strain expressing various Hxts, it is impossible to evaluate the effects of drugs on the substrate specificity of individual Hxts, although it is easy to monitor the growth of the *hxt*^{0} mutant harboring only a single *HXT* gene. As shown in Figure 6D (left), in the absence of TC, the HXT1m and HXT2m strains grew on a medium containing glucose, fructose, and mannose, but not galactose, as a solo carbon source. This reflects the fact that Hxt1 and Hxt2 are unable to transport galactose (Leandro *et al.* 2009). Both strains were sensitive to 2.5 mM TC in the presence of 2% glucose or fructose but not in the presence of mannose; furthermore, these sensitivities were alleviated by additional monosaccharides (4–8%) (Figure 6D). The HXT1m strain was sensitive to 3.5 mM TC, and this effect was alleviated by additional mannose (4–8%) (Figure 6B). These observations suggest that administration of TC effectively inhibits the transport of glucose and fructose rather than mannose in Hxt1 and Hxt2 irrespective of the difference in their substrate affinities.

Interestingly, in the presence of 2% glucose, additional galactose (2–4%) effectively alleviated TC sensitivity in the HXT1m strain, but it had only a slight effect in the HXT2m strain (Figure 6D, right). Thus, the galactose-induced alleviation pattern depends on the properties of individual Hxts rather than on other systems. Because both Hxts are unable to import galactose, excessive amounts of galactose might stimulate glucose import in the presence of TC. Alternatively, the coexistence of glucose might stimulate galactose import in these Hxts. In the latter case, galactose metabolism would contribute to the alleviation. However, addition of 2-deoxygalactose (dGal), a nonmetabolizable galactose analogue, also alleviated the TC sensitivity of the HXT1m strain in the presence of 2% glucose (Figure 6E, +2% dGal). Thus, additional galactose likely would stimulate glucose import. Similar alleviation of TC effects was observed following the addition of OMG (Figure 6E, +4% OMG). In the HXT1s strain, alleviation of TC sensitivity was not apparent with additions of OMG, galactose, or dGal, although slight alleviation was observed in the presence of 6% glucose (+4% Glc) following prolonged incubation for 5 days (Figure 6E, 1s). These results indicate that alleviation of TC sensitivity by the addition of nonmetabolizable hexose analogues also depends on the amount of Hxt1 rather on other systems such as the Gpr1-Gpa2 and Rgt2-Snf3 sensors.

Addition of 4% OMG, but not 4% dGal, alleviated the TC sensitivity of the HXT1m strain (Figure 6E, 1m). This difference may have arisen because high concentrations of nonimportable galactose preferentially mask the

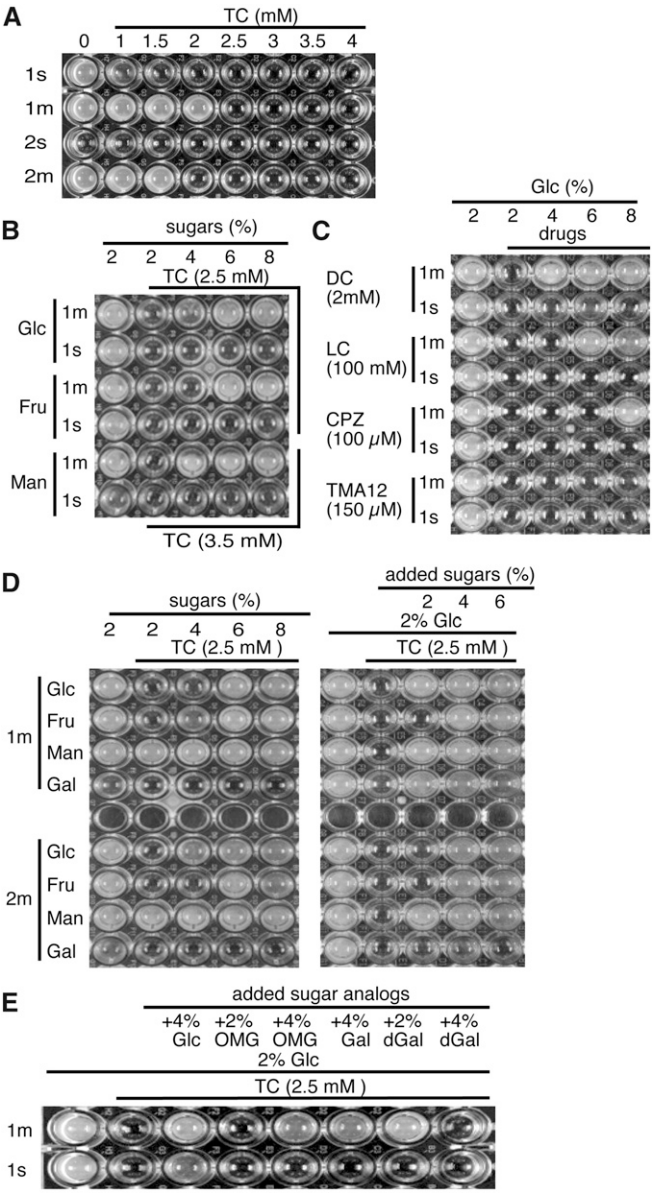

Figure 6 The effects of drugs and sugars on the growth of *hxt*^{0} mutants harboring only a *HXT* gene. The *hxt*^{0} mutants harboring pHXT1s (1s), pHXT1m (1m), pHXT2s (2s), and pHXT2m (2m) were precultured in SMal-Ura, respectively, and then grown in YPD for 4–5 hr. A. These strains were incubated on 96-well plates containing YPD (pH 6.0) supplemented with TC at the indicated concentrations (horizontal axis) for 3 days at 25°. (B) The *hxt*^{0} mutants (1m and 1s) were incubated in wells containing YP (pH 6.0) supplemented with the indicated sugars (vertical axis) and TC at the indicated concentrations (horizontal axis) for 3 days at 25°. (C) The *hxt*^{0} mutants (1m and 1s) were incubated in wells containing YP (pH 6.0) supplemented with the drugs (vertical axis) and glucose (horizontal axis) at the indicated concentrations for 3 days at 25°. (D) The *hxt*^{0} mutants (1m and 2m) were incubated in wells containing YP (left) and YPD (right) (pH 6.0) supplemented with the indicated monosaccharides (vertical axis) and TC at the indicated concentrations (horizontal axis) for 3 days at 25°. (E) The *hxt*^{0} mutants (1m and 1s) were incubated in wells containing YPD (pH 6.0) supplemented with additional glucose, OMG, galactose, dGal, and TC at the indicated concentrations (horizontal axis) for 5 days at 25°.

hexose-recognition portions of Hxt1, resulting in interference of the glucose import, but transportable OMG does not. These observations suggest that Hxt1, defective in galactose transport, can recognize galactose but not transport it. In other words, additional galactose might stimulate glucose import by affecting the hexose-recognition portions of Hxt1.

Amphiphilic clinical drugs, nonspecifically distributed in various membranes, affect Hxts on the plasma membrane

According to the protein theory, local anesthetics and phenothiazines would inhibit hexose transport via direct interaction with Hxts; however, according to the lipid theory, these drugs would indirectly inhibit hexose transport via direct interaction with membranes. To examine these possibilities, we observed the intracellular localization of phenothiazines. The fluorescence of phenothiazines was detected by UV excitation (330–385 nm) as blue-like signals for CPZ (De Filippi *et al.* 2007) and yellow-like signals for TFZ, although both colors rapidly changed to a white-like color possibly because of UV degradation. Similar fluorescence signals for both CPZ and TFZ were distributed in various membranes, including vacuole-like structures (Figure 7A, top), irrespective of their structural differences. The signals were observed just after treatment with the phenothiazines, which was apparently different from the slow staining of vacuoles by FM4-64 dye (data not shown). This suggests that penetration of the phenothiazines is a rapid process without endocytotic trafficking. Similar localizations were observed following treatments with perphenazine (PPZ), thioridazine (TRZ), and fluphenazine (FPZ) as blue-like, blue-white-like, and yellow-like signals, respectively. These observations suggest that chloride (CPZ and PPZ), the methylthio group (TRZ), and the trifluoromethyl group (TFZ and FPZ) in their phenothiazine rings contribute to the color differences (data not shown). Thus, the localization to membranes is due to the common structure of phenothiazines rather than the individual structures. These observations indicate that the phenothiazines with cationic amphiphilic structures nonspecifically interact with membranes, possibly via the amphiphilic intercalation along the orientation of the membrane phospholipids.

In comparison, GFP-tagged Hxt2 and Hxt1 were specifically localized in the plasma membrane (Figure 7A, bottom, and Figure 7B, ctrl), as reported previously (Yoshida *et al.* 2012). The difference in these localizations indicates that phenothiazines do not interact only with Hxts. In cells with reduced glucose uptake caused by treatment with 0.4 mM CPZ for 30 min (Figure 2A), the Hxt1-GFP signals were retained at the plasma membrane (Figure 7B), which indicates that the inhibition of glucose uptake is not due to delocalization of Hxt1. If CPZ were anchored at the plasma membrane via interactions with Hxts and other membrane proteins, according to the protein theory, a small increase in CPZ would not affect membrane structures. However, at 1 mM, the CPZ signals on the membranes were lost and

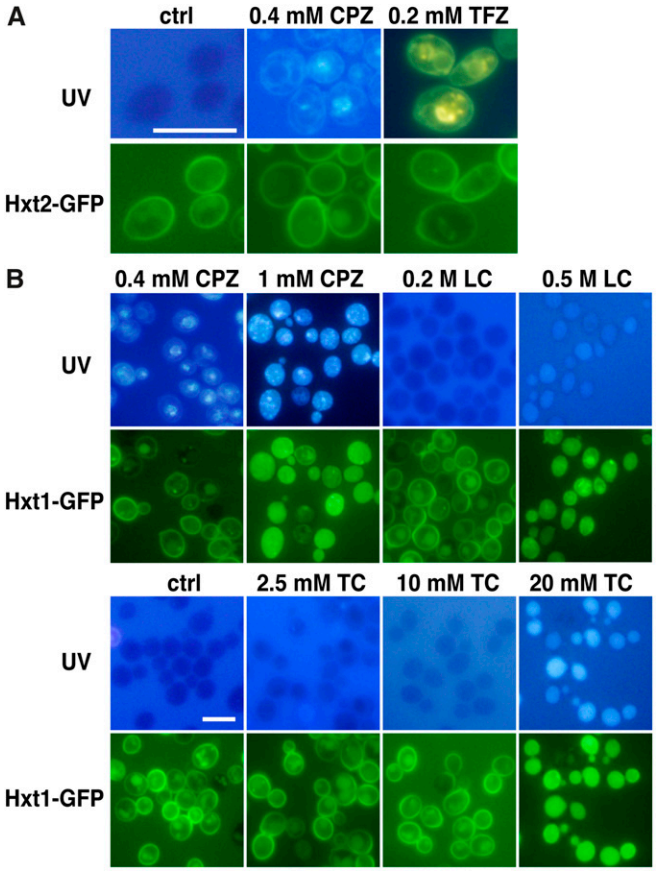

Figure 7 Colocalization of fluorescence signals for phenothiazines and Hxts. (A) BY4741 cells expressing Hxt2-GFP (YYU609) grown in YPD (pH 6.0) were treated with 0.4 mM CPZ and 0.2 mM TFZ for 30 min at 25°. The fluorescence signals for phenothiazine excited by UV irradiation are shown in the upper panels, and Hxt2-GFP signals are shown in the lower panels. (B) BY4741 cells expressing Hxt1-GFP (YYU608) grown in YPD (pH 6.0) were treated with CPZ, LC, and TC at the indicated concentrations. The fluorescence signals excited by UV irradiation are shown in the upper panels, and Hxt1-GFP signals are shown in the lower panels. The untreated cells are shown in each panel (ctrl). Bar, 10 μm.

distributed as dot-like structures; concomitantly, Hxt1-GFP signals on the plasma membrane also were lost. Because this concentration induces cell lysis, as judged by ALP activity (Uesono *et al.* 2011), CPZ at 1 mM destroys membranes via the surfactant-like activity of the amphiphilic structure, and it thereby delocalizes Hxt1 from the plasma membrane. Thus, CPZ directly and nonspecifically interacts with various membranes rather than with membrane proteins.

LC and TC also have amphiphilic structures, although they do not have the structures for fluorescence (Uesono *et al.* 2011). At concentrations that reduce glucose uptake (*i.e.*, 0.2 M LC, 0.5 hr; 2.5 mM TC, 4 hr; and 10 mM TC, 0.5 hr) (Figure 2), the Hxt1-GFP signals were retained at the plasma membrane (Figure 7B), although apparent permeabilization was observed following treatment with 10 mM TC (Figure 3C, left). Thus, the inhibition of glucose uptake, which is caused by the conditions, is not due to delocalization of Hxt1. The intrinsic fluorescence signals were observed by

UV excitation, and the Hxt1-GFP signals were lost from the plasma membrane at high concentrations that induced cell lysis (*i.e.*, 0.5 M LC, 0.5 hr, and 20 mM TC, 0.5 hr) (Uesono *et al.* 2011). These effects were likely the result of membrane destruction at high concentrations caused by surfactant-like activity based on the amphiphilic structures of local anesthetics, as observed with 1 mM CPZ. These results suggest that the amphiphilic clinical drugs, which are distributed nonspecifically in various membranes, indirectly and incidentally interact with the Hxts specifically localized on the plasma membrane rather than anchoring the drugs by Hxts or other membrane proteins and that they thereby inhibit the function of Hxts at low concentrations.

Discussion

Cationic amphiphilic compounds nonspecifically interact with whole-cell membranes

The nonspecific interaction of local anesthetics and phenothiazines with membranes is not specific to yeast cells because similar membrane interactions have been proposed following morphologic analysis of erythrocyte cells (Deuticke 1968; Sheetz and Singer 1974). These interactions simply may be due to the intercalation of the amphiphilic drugs along the orientation of amphiphilic phospholipids in the lipid bilayer. Even if these drugs have the potential to interact with specific proteins at low concentrations, the nonspecific interaction between the drugs and membranes would remain unchanged because the amphiphilic structures do not change with concentration. Therefore, we suggest that the action mechanism of these amphiphilic drugs can be understood based on the lipid theory.

Protein theory is based on several observations, including the cutoff phenomenon of long-chain alcohols (Franks and Lieb 1990). Cutoff is the unresolved phenomenon by which long-chain compounds with more than C_{12} carbons, such as alcohols and QACs, lose their anesthetic activity in animals (Pringle *et al.* 1981; Curtis and Scurlock 1981). Thus, cutoff is an apparent contradiction of the Meyer-Overton rule. To explain the cutoff and the luciferase inhibition by anesthetics, protein theory assumes that the target proteins, such as neurotransmitter receptors and ion channels, might have anesthetic-binding pockets of limited size as their hydrophobic sites that are unable to fit long-chain compounds larger than the cutoff length. However, the cutoff of long-chain alcohols was observed in the growth-inhibitory activity in microorganisms, indicating that the phenomenon is not specific for anesthesia of animals (Kato and Shibasaki 1980; Kubo *et al.* 1995). Pharmacologic analysis of yeast has revealed that cationic TMAs, which have anesthetic activity in animals (Curtis and Scurlock 1981), do not lose their inhibitory activities, *i.e.*, actin polarization and translation initiation, even if they have long alkyl chains (C_6–C_{18}). This indicates that the anesthetic-binding pocket of limited size does not exist (Uesono *et al.* 2011). In addition, the real potencies of TMAs found by escaping cutoff at the lower concentrations proportionally increase (*i.e.*, IC_{50} values decrease) with their carbon number and peak at C_{16}, which is the average length of yeast membrane fatty acids (van der Rest *et al.* 1995). This suggests that an interaction exists between long-chain compounds and one side of the membrane lipid bilayer (Uesono *et al.* 2011). The lipids of the plasma membrane are usually distributed asymmetrically. The inner leaflet of the yeast plasma membrane is enriched in phosphatidylethanolamine (PE), phosphatidylinositol (PI), and phosphatidylserine (PS) (van der Rest *et al.* 1995); this composition is similar to that of erythrocyte membranes (Op den Kamp 1979). Morphologic studies of erythrocytes suggest that the positively charged cationic amphiphiles, including local anesthetics and phenothiazines, preferentially intercalate into the inner leaflet enriched in the negative-charged PI and PS (Deuticke 1968; Sheetz and Singer 1974). Thus, cationic amphiphiles would preferentially and nonspecifically intercalate into the inner leaflets of the yeast lipid bilayer via electrostatic interactions with anionic phospholipids (Figure 8).

A mechanism that motivates nonspecific interaction between drugs and membranes induces specific glucose starvation

The nonspecific interaction of the cationic amphiphiles with the membrane is considered to inhibit the function of numerous proteins on membranes, and this results in various phenotypes rather than a specific phenotype. However, our results indicate that the cationic amphiphiles induce specific glucose starvation via inhibition of Hxt function. This apparently contradicts the various phenotypes. To explain this contradiction, we propose two models (Figure 8, A and B). In one model, we explain how the nonspecific interaction inhibits the function of Hxts (Figure 8A). An alternating conformation model has been proposed previously to explain the mechanism of facilitated glucose transport (Gorga and Lienhard 1981; Oka *et al.* 1990). In this model, glucose is selectively transported across membranes via oscillated changes between outward- and inward-facing conformations. Nonspecific intercalation of amphiphiles with membrane would inhibit this oscillation. However, in contrast to the effects caused by cationic TMA12, anionic SDS does not inhibit translation initiation (Uesono *et al.* 2008), and additional glucose does not alleviate the SDS-associated growth inhibition (Figure 3A). Therefore, anionic amphiphiles, which are considered to intercalate into outer leaflets (Deuticke 1968), are unlikely to induce glucose starvation. This simply suggests that cationic amphiphiles efficiently inhibit Hxts by penetrating into the open space of the oscillation area at the inner leaflet, but anionic amphiphiles do not because the area at the outer leaflets has no space if the Hxts importing extracellular hexoses usually exist as the outward-facing form (Figure 8A, low drugs). This implies that compounds with widely varying structures, other than the drugs used in this study, might induce glucose starvation if they penetrate into inner leaflets.

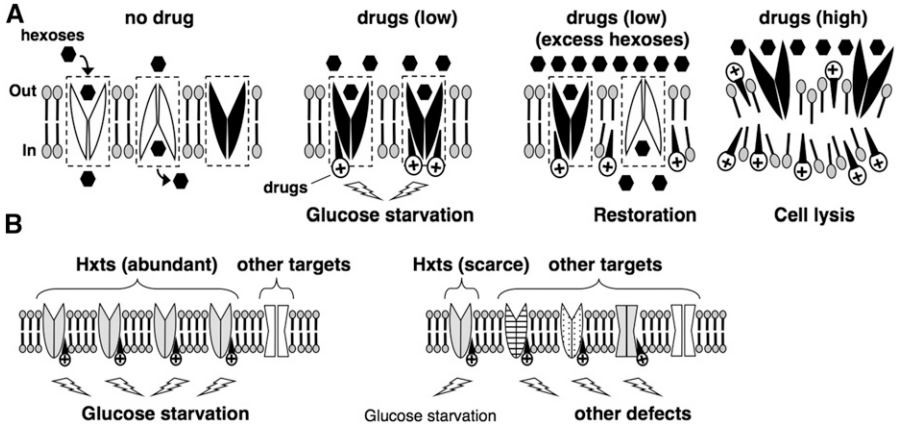

Figure 8 Models for the preferential inhibition of Hxts caused by nonspecific interaction between cationic amphiphiles and membranes. (A) Hexoses are selectively transported across the plasma membrane via oscillated changes in the Hxts between outward- and inward-facing conformations (no drug). Active Hxts transporting hexoses are indicated as white shapes, and inactive Hxts without transporting hexoses are indicated as black shapes. The dotted boxes indicate the oscillation area for the conformational change of Hxts. At low concentrations, cationic amphiphilic drugs (*e.g.*, local anesthetics, phenothiazines, and cationic surfactants) nonspecifically intercalate into the inner leaflet of membranes (drugs, low). When the drugs penetrate into the oscillation area of Hxts, their structural changes are prevented as the outward-facing configuration (black shapes), resulting in glucose starvation. Additional hexoses stimulate the oscillation of Hxts by efficient interaction with hexoses (drugs, low + excess hexoses) and thus prevent drug penetration into the oscillating area, thereby conferring resistance to drugs (white shapes). Once the drugs penetrate into the oscillating area, the stuck Hxts no longer oscillate efficiently, even in the presence of additional hexose (black shapes). Increasing the drug concentrations destroys membranes by excessively penetrating into the lipid layer, and thus Hxts do not exist in the plasma membrane and lose their function (drugs, high). (B) A certain concentration of cationic amphiphiles preferentially inhibits the function of abundant Hxts in plasma membrane (left). In the case of scarce Hxts, the drugs inhibit various targets, thereby diminishing the preference of Hxts as a drug target (right).

The rate-limiting step for TC resistance was the amount of substrate for Hxts rather than the number of Hxts themselves (Figure 5, B and C). This implies that TC resistance is conferred by Hxts that are actively oscillated by transporting hexose but not by nonoscillated Hxts that do not transport hexose (Figure 8A, no drugs, white and black shapes). Thus, additional hexose would lead to increasingly efficient oscillation of Hxts by maintaining a substrate supply and thus would prevent the penetration of the drugs into the actively oscillating area, which, in turn, would confer resistance to the drugs (Figure 8A, excess hexoses, white shapes). However, once the drugs penetrate into the oscillating area, the transporters that are stuck no longer oscillate efficiently, even if excessive amounts of glucose are added (Figure 8A, excess hexoses, black shapes). Therefore, the state of glucose uptake would depend on the first attack, either of the oscillation area by the drugs or of the transporters by the additional glucose. This assumption is supported by the observation that the state of actin depolarization depends on the first treatment, either of TC or of additional glucose (Figure 4A). Eventually, the drugs would penetrate into the oscillation area with consumption of glucose even if it were in excessive amounts. This is supported by the fact that actin tended to gradually depolarize in the cell pretreated with 6% glucose (Figure 4A). This mechanism for drug resistance by stimulation of oscillatory change would be applicable to numerous compounds that penetrate the membrane. Therefore, this mechanism might provide insight into multidrug resistance in cells that actively assimilate glucose via Hxts, such as cancer cells (Phelps 2000). At higher concentrations, these amphiphilic drugs would destroy the membrane by excessively penetrating into the lipid layers, as observed in erythrocytes, model membranes, and yeast (Seeman 1972; Kitagawa *et al.* 2004; Uesono *et al.* 2011) (Figure 7B); thereafter, Hxts no longer exist (Figure 8A, high drugs), and additional glucose cannot therefore alleviate the defects (Figure 3, C and D, 10 mM TC).

We acknowledge that the aforementioned model alone cannot explain the specificity of Hxts because the mechanism is applicable to other transporters/channels that severely change the structures on membranes (Yan 2015). Thus, another model is also required (Figure 8B). *S. cerevisiae* has the largest number of major facilitator superfamily (MFS) transporters of any organism; these transporters move their substrates by passive, energy-independent facilitated diffusion (Pao *et al.* 1998). Of the MFS transporters, the hexose transporter is the largest family, encoded by 18 genes and 2 sensors (Ozcan and Johnston 1999). Because several *HXT* genes are highly expressed in media containing sufficient amounts of glucose, Hxts likely would be abundant in the plasma membrane of the WT strain. In this study, excessive amounts of hexoses alleviated drug sensitivity in the HXT1m strain but not in the HXT1s strain (Figure 6, B and C). This indicates that glucose starvation is responsible for drug sensitivity in the presence of high, but not low, levels of Hxt1, which is a gene dose–dependent biphasic behavior. In other words, cationic amphiphiles distributed nonspecifically in membranes would preferentially inhibit abundant Hxts in a WT strain with high expression of various *HXT* genes, and this would induce glucose starvation as a preferential phenotype. Thus, this effect can be alleviated by additional hexoses (Figure 8B, left). In the presence of small numbers of Hxts, the cationic amphiphiles would equally inhibit the functions of other membrane targets as well as Hxts, which would result in various defects. This effect, therefore, would not be alleviated by additional hexoses only (Figure 8B, right). If this were a convincing mechanism, broadening the drug penetration area by increasing the concentration would induce various defects; *i.e.*, it would show drug dose-dependent

biphasic behavior. Indeed, this is confirmed by the fact that TC induces the eIF2α phosphorylation sensing starvation of amino acids at high concentrations only (Araki *et al.* 2015). Alternatively, Hxts might have a special cytoplasmic domain where the oscillation is easily inhibited by the nonspecific interaction of drugs with the membrane. However, this latter case cannot explain the aforementioned biphasic behaviors because Hxts alone are inhibited irrespective of the amounts of Hxts and drugs. In summary, these two models would explain a possible mechanism by which a nonspecific interaction between cationic amphiphiles and membranes preferentially induces specific glucose starvation and leads to similar responses.

Inhibitory effects of clinical drugs on glucose transport in animals

The function of Hxts is highly conserved from yeast to animals (Kasahara and Kasahara 1997; Wieczorke *et al.* 2003). Administration of volatile and local anesthetics is known to increase blood glucose levels in animals and humans (Diltoer and Camu 1988; Nakamura *et al.* 2001). Antipsychotic drugs, including phenothiazines, are also known to induce hyperglycemia irrespective of whether the drugs are typical or atypical (Haupt and Newcomer 2001). These facts suggest that administration of these clinical drugs inhibits glucose transport at a cellular level as a common effect and that this increases blood glucose levels in animals. In addition, the apparent inhibition of glucose uptake is observed in human erythrocytes and brain during administration of volatile anesthetics (Salah *et al.* 1982; Alkire *et al.* 1997), as well as in PC12 cells following treatment with phenothiazines (Dwyer *et al.* 1999). With our findings, these facts suggest that anesthetics and antipsychotic phenothiazines inhibit the function of Hxts in animals in a similar manner irrespective of the structural difference of the drugs. According to our theory, the nonspecific interaction of the cationic drugs with membrane would preferentially affect the most abundant transporters/channels/receptors with structural changes on the membrane in tissues. For example, because glucose is used efficiently in the brain in all the human tissues (Phelps 2000), the inhibitory effects caused by anesthetics and phenothiazines would preferentially appear on glucose transporters highly expressed in the brain. Glucose starvation in the brain, compulsively caused by these drugs, might account for the loss of consciousness during anesthesia, similar to hypoglycemic comas observed in diabetic patients (Languren *et al.* 2013). In tissues with insufficient glucose transporters, phenotypes other than glucose starvation would appear.

Alleviation of drug-induced toxicity: Anesthetics and phenothiazines are known to induce cytotoxicity in mammalian cells at clinically relevant concentrations, which is considered to correlate with drug-induced neurodegenerative diseases (Gil-Ad *et al.* 2004; Werdehausen *et al.* 2009; Stratmann 2011). The viability of yeast cells also gradually decreased, without cell lysis, following exposure to TC at low concentrations (Figure 4B), as observed in long-term treatment with isoflurane (Keil *et al.* 1996). This indicates that these anesthetics lead to irreversible toxic effects even in yeast cells. This effect is possibly attributable to the aberrant glucose-starvation-mimetic state, which is compulsively caused by the drugs being distributed to various membranes (Figure 7). Our results suggest that the aberrant state is caused by inhibition of an unknown survival process linked to glucose utilization (Figure 6B). The respiration system might be a candidate because it is required for homeostasis after glucose deprivation (Uesono *et al.* 2004). Drug penetration into both mitochondrial and plasma membranes might generate toxicity as a result of irregular inhibition of both respiration and glucose uptake. At the tissue level in rats, additional glucose alleviates the neurotoxicity induced by TC (Fukushima *et al.* 2011), similar to our observations in yeast (Figure 4B). Thus, the toxicity-alleviation mechanism might be similar between yeast and rats. If the mechanisms for drug toxicity are also similar in humans, alleviation of the glucose-starvation-mimetic state by the administration of excessive amounts of hexoses, insulin, or both might be effective for avoiding the adverse effects induced by anesthetics in the brain, such as postoperative cognitive dysfunction in normal patients (Moller *et al.* 1998), which has already been performed as the tight glycemic control for other purposes (Malmberg *et al.* 1995; van den Berghe *et al.* 2001).

Acknowledgments

We thank Y. Inoue, W. Nomura, and K. Yamada of Kyoto University; T. Kasahara of Teikyo University; E. Boles of Goethe University; and Y. Osakabe of Tokushima University for providing plasmids and strains and M. Tanikawa of University of Tokyo for help on the radioisotope experiments.

Literature Cited

Antkowiak, B., 2001 How do general anaesthetics work? Naturwissenschaften 88: 201–213.

Alkire, M. T., R. J. Haier, N. K. Shah, and C. T. Anderson, 1997 Positron emission tomography study of regional cerebral metabolism in humans during isoflurane anesthesia. Anesthesiology 86: 549–557.

Araki, T., A. Toh-e, Y. Kikuchi, C. K. Watanabe, T. Hachiya *et al.*, 2015 Tetracaine, a local anesthetic, preferentially induces translational inhibition with processing body formation rather than phosphorylation of eIF2α in yeast. Curr. Genet. 61: 43–53.

Ashe, M. P., S. K. De Long, and A. B. Sachs, 2000 Glucose depletion rapidly inhibits translation initiation in yeast. Mol. Biol. Cell 11: 833–848.

Banerjee, D., and C. M. Redman, 1977 Effect of local anesthetics on plasma protein secretion by rat hepatocytes. Biochim. Biophys. Acta 500: 49–60.

Bruce, D. L., 1975 Halothane inhibition of RNA and protein synthesis of PHA-treated human lymphocytes. Anesthesiology 42: 11–14.

Cheng, Q., and C. A. Michels, 1989 The maltose permease encoded by the *MAL61* gene of *Saccharomyces cerevisiae* exhibits

both sequence and structural homology to other sugar transporters. Genetics 123: 477–484.
Curtis, B. M., and J. E. Scurlock, 1981 The mechanism of action of local anesthesia by tetraethylammonium derivatives. Anesthesiology 54: 270–277.
De Filippi, L., M. Fournier, E. Cameroni, P. Linder, C. De Virgilio *et al.*, 2007 Membrane stress is coupled to a rapid translational control of gene expression in chlorpromazine-treated cells. Curr. Genet. 52: 171–185.
Delley, P. A., and M. N. Hall, 1999 Cell wall stress depolarizes cell growth via hyperactivation of *RHO1*. J. Cell Biol. 147: 163–174.
Deuticke, B., 1968 Transformation and restoration of biconcave shape of human erythrocytes induced by amphiphilic agents and changes of ionic environment. Biochim. Biophys. Acta 163: 494–500.
Diltoer, M., and F. Camu, 1988 Glucose homeostasis and insulin secretion during isoflurane anesthesia in humans. Anesthesiology 68: 880–886.
Dwyer, D. S., H. B. Pinkofsky, Y. Liu, and R. J. Bradley, 1999 Antipsychotic drugs affect glucose uptake and the expression of glucose transporters in PC12 cells. Prog. Neuropsychopharmacol. Biol. Psychiatry 23: 69–80.
Franks, N. P., and W. R. Lieb, 1990 Mechanisms of general anesthesia. Environ. Health Perspect. 87: 199–205.
Fukushima, S., T. Takenami, S. Yagishita, T. Nara, and H. Okamoto, 2011 Hyperbaric glucose solution lessens neurotoxicity of intrathecal tetracaine in rats. J. Jpn. Soc. Pain Clin. 18: 34–39.
Gancedo, J. M., 2008 The early steps of glucose signalling in yeast. FEMS Microbiol. Rev. 32: 673–704.
Gietz, R. D., and A. Sugino, 1988 New yeast–Escherichia coli shuttle vectors constructed with in vitro mutagenized yeast genes lacking six-base pair restriction sites. Gene 74: 527–534.
Gil-Ad, I., B. Shtaif, Y. Levkovitz, M. Dayag, E. Zeldich *et al.*, 2004 Characterization of phenothiazine-induced apoptosis in neuroblastoma and glioma cell lines-Clinical relevance and possible application for brain-derived tumors. J. Mol. Neurosci. 22: 189–198.
Gorga, F. R., and G. E. Lienhard, 1981 Equilibria and kinetics of ligand binding to the human erythrocyte glucose transporter: evidence for an alternating conformation model for transport. Biochemistry 20: 5108–5113.
Guthrie, C., and G. R. Fink, 1991 *Guide to Yeast Genetics and Molecular Biology* (Methods in Enzymology, Vol. 194). Academic Press, New York.
Haupt, D. W., and J. W. Newcomer, 2001 Hyperglycemia and antipsychotic medications. J. Clin. Psychiatry 27: 15–26.
Heys, S. D., A. C. Norton, C. R. Dundas, O. Eremin, K. Ferguson *et al.*, 1989 Anaesthetic agents and their effect on tissue protein synthesis in the rat. Clin. Sci. 77: 651–655.
Horber, F. F., S. Krayer, K. Rehder, and M. W. Haymond, 1988 Anesthesia with halothane and nitrous oxide alters protein and amino acid metabolism in dogs. Anesthesiology 69: 319–326.
Kasahara, T., and M. Kasahara, 1997 Characterization of rat Glut4 glucose transporter expressed in the yeast *Saccharomyces cerevisiae*: comparison with Glut1 glucose transporter. Biochim. Biophys. Acta 1324: 111–119.
Kasahara, T., and M. Kasahara, 2003 Transmembrane segments 1, 5, 7 and 8 are required for high-affinity glucose transport by *Saccharomyces cerevisiae* Hxt2 transporter. Biochem. J. 372: 247–252.
Kato, N., and I. Shibasaki, 1980 The antimicrobial characteristics of 1-alkanols. J. Antibact. Antifung. Agents 8: 325–331.
Keil, R. L., D. Wolfe, T. Reiner, C. J. Peterson, and J. L. Riley, 1996 Molecular genetic analysis of volatile-anesthetic action. Mol. Cell. Biol. 16: 3446–3453.
Kitagawa, N., M. Oda, and T. Totoki, 2004 Possible mechanism of irreversible nerve injury caused by local anesthetics: detergent properties of local anesthetics and membrane disruption. Anesthesiology 100: 962–967.
Kubo, I., H. Muroi, and A. Kubo, 1995 Structural functions of antimicrobial long-chain alcohols and phenols. Bioorg. Med. Chem. 3: 873–880.
Kumar, R. V., R. Panniers, A. Wolfman, and E. C. Henshaw, 1991 Inhibition of protein synthesis by antagonists of calmodulin in Ehrlich ascites tumor cells. Eur. J. Biochem. 195: 313–319.
Laborit, H., P. Huguenard, and R. Alluaume, 1952 Un noveau stabilisateur végétatif (le 4560 RP). Presse Med. 60: 206–208.
Languren, G., T. Montiel, A. Julio-Amilpas, and L. Massieu, 2013 Neuronal damage and cognitive impairment associated with hypoglycemia: an integrated view. Neurochem. Int. 63: 331–343.
Leandro, M. J., C. Fonseca, and P. Gonçalves, 2009 Hexose and pentose transport in ascomycetous yeasts: an overview. FEMS Yeast Res. 9: 511–525.
Liang, H., and R. F. Gaber, 1996 A novel signal transduction pathway in *Saccharomyces cerevisiae* defined by Snf3-regulated expression of *HXT6*. Mol. Biol. Cell 7: 1953–1966.
Malmberg, K., L. Rydén, S. Efendic, J. Herlitz, P. Nicol *et al.*, 1995 Randomized trial of insulin-glucose infusion followed by subcutaneous insulin treatment in diabetic patients with acute myocardial infarction (DIGAMI study): effects on mortality at 1 year. J. Am. Coll. Cardiol. 26: 57–65.
Meyer, H., 1899 Zur theorie der alkoholnarkose. Arch. Exp. Pathol. Pharmakol. 42: 109–118.
Moller, J. T., P. Cluitmans, L. S. Rasmussen, P. Houx, H. Rasmussen *et al.*, 1998 Long-term postoperative cognitive dysfunction in the elderly ISPOCD1 study. ISPOCD investigators. International Study of Post-Operative Cognitive Dysfunction. Lancet 351: 857–861.
Mozrzymas, J. W., A. Barberis, K. Michalak, and E. Cherubini, 1999 Chlorpromazine inhibits miniature GABAergic currents by reducing the binding and by increasing the unbinding rate of GABAA receptors. J. Neurosci. 19: 2474–2488.
Nakamura, Y., K. Matsumura, K. Miura, H. Kurokawa, I. Abe *et al.*, 2001 Cardiovascular and sympathetic responses to dental surgery with local anesthesia. Hypertens. Res. 24: 209–214.
Ogata, N., M. Yoshii, and T. Narahashi, 1989 Psychotropic drugs block voltage-gated ion channels in neuroblstoma cells. Brain Res. 474: 140–144.
Oka, Y., T. Asano, Y. Shibasaki, J. L. Lin, K. Tsukuda *et al.*, 1990 C-terminal truncated glucose transporter is locked into an inward-facing form without transport activity. Nature 345: 550–553.
Op den Kamp, J. A. F., 1979 Lipid asymmetry in membranes. Annu. Rev. Biochem. 48: 47–71.
Ozcan, S., and M. Johnston, 1999 Function and regulation of yeast hexose transporters. Microbiol. Mol. Biol. Rev. 63: 554–569.
Palmer, L. K., J. L. Shoemaker, B. A. Baptiste, D. Wolfe, and R. L. Keil, 2005 Inhibition of translation initiation by volatile anesthetics involves nutrient-sensitive GCN-independent and -dependent processes in yeast. Mol. Biol. Cell 16: 3727–3739.
Pao, S. S., I. T. Paulsen, and M. H. Jr. Saier, 1998 Major facilitator superfamily. Microbiol. Mol. Biol. Rev. 62: 1–34.
Phelps, M. E., 2000 Positron emission tomography provides molecular imaging of biological processes. Proc. Natl. Acad. Sci. USA 97: 9226–9233.
Pringle, M. J., K. B. Brown, and K. W. Miller, 1981 Can the lipid theories of anesthesia account for the cutoff in anesthetic potency in homologous series of alcohols? Mol. Pharmacol. 19: 49–55.

Prozialeck, W. C., and B. J. Weiss, 1982 Inhibition of calmodulin by phenothiazines and related drugs: structure-activity relationships. Pharmacol. Exp. Ther. 222: 509–516.
Raghupathy, E., N. A. Peterson, and C. M. McKean, 1970 Effects of phenothiazines on in vitro cerebral protein synthesis. Biochem. Pharmacol. 19: 993–1000.
Salah, K. M., K. K. Hampton, and J. B. Findlay, 1982 The effects of general anaesthetics on glucose and phosphate transport across the membrane of the human erythrocyte. Biochim. Biophys. Acta 688: 163–168.
Seeman, P., 1972 The membrane actions of anesthetics and tranquilizers. Pharmacol. Rev. 24: 583–655.
Sheetz, M. P., and S. J. Singer, 1974 Biological membranes as bilayer couples: a molecular mechanism of drug-erythrocyte interactions. Proc. Natl. Acad. Sci. USA 71: 4457–4461.
Snyder, S. H., S. P. Banerjee, H. I. Yamamura, and D. Greenburg, 1974 Drugs, neurotransmitters and schizophrenia. Science 184: 1243–1253.
Stratmann, G., 2011 Neurotoxicity of anesthetic drugs in the developing brain. Anesth. Analg. 113: 1170–1179.
Toh-e, A., H. Nakamura, and Y. Oshima, 1976 A gene controlling the synthesis of non-specific alkaline phosphatase in *Saccharomyces cerevisiae*. Biochim. Biophys. Acta 428: 182–192.
Uesono, Y., 2009 Environmental stresses and clinical drugs paralyze a cell. Commun. Integr. Biol. 2: 275–278.
Uesono, Y., and A. Toh-e, 2002 Transient inhibition of translation initiation by osmotic stress. J. Biol. Chem. 277: 13848–13855.
Uesono, Y., M. P. Ashe, and A. Toh-e, 2004 Simultaneous yet independent regulation of actin cytoskeletal organization and translation initiation by glucose in *Saccharomyces cerevisiae*. Mol. Biol. Cell 15: 1544–1556.
Uesono, Y., T. Araki, and A. Toh-e, 2008 Local anesthetics, antipsychotic phenothiazines, and cationic surfactants shut down intracellular reactions through membrane perturbation in yeast. Biosci. Biotechnol. Biochem. 72: 2884–2894.
Uesono, Y., A. Toh-e, Y. Kikuchi, and I. Terashima, 2011 Structural analysis of compounds with actions similar to local anesthetics and antipsychotic phenothiazines in yeast. Yeast 28: 391–404.
Urban, B. W., M. Bleckwenn, and M. Barann, 2006 Interactions of anesthetics with their targets: non-specific, specific or both? Pharmacol. Ther. 111: 729–770.
van den Berghe, G., P. Wouters, F. Weekers, C. Verwaest, F. Bruyninckx *et al.*, 2001 Intensive insulin therapy in critically ill patients. N. Engl. J. Med. 345: 1359–1367.
van der Rest, M. E., A. H. Kamminga, A. Nakano, Y. Anraku, B. Poolman *et al.*, 1995 The plasma membrane of *Saccharomyces cerevisiae*: structure, function, and biogenesis. Microbiol. Rev. 59: 304–322.
Wang, D., N. V. Vo, G. A. Sowa, R. A. Hartman, K. Ngo *et al.*, 2011 Bupivacaine decreases cell viability and matrix protein synthesis in an intervertebral disc organ model system. Spine J. 11: 139–146.
Werdehausen, R., S. Fazeli, S. Braun, H. Hermanns, F. Essmann *et al.*, 2009 Apoptosis induction by different local anaesthetics in a neuroblastoma cell line. Br. J. Anaesth. 103: 711–718.
Wessels, S., and H. Ingmer, 2013 Modes of action of three disinfectant active substances: a review. Regul. Toxicol. Pharmacol. 67: 456–467.
Wieczorke, R., S. Dlugai, S. Krampe, and E. Boles, 2003 Characterisation of mammalian GLUT glucose transporters in a heterologous yeast expression system. Cell. Physiol. Biochem. 13: 123–134.
Yan, N., 2015 Structural biology of the major facilitator superfamily transporters. Annu. Rev. Biophys. 44: 257–283.
Yoshida, A., D. Wei, W. Nomura, S. Izawa, and Y. Inoue, 2012 Reduction of glucose uptake through inhibition of hexose transporters and enhancement of their endocytosis by methylglyoxal in *Saccharomyces cerevisiae*. J. Biol. Chem. 287: 701–711.

Communicating editor: O. Cohen-Fix